

Article

Research on Sea State Signal Recognition Based on Beluga Whale Optimization–Slope Entropy and One Dimensional–Convolutional Neural Network

Yuxing Li ^{1,2,*} , Zhaoyu Gu ¹ and Xiumei Fan ¹

¹ School of Automation and Information Engineering, Xi'an University of Technology, Xi'an 710048, China

² Shaanxi Key Laboratory of Complex System Control and Intelligent Information Processing, Xi'an University of Technology, Xi'an 710048, China

* Correspondence: liyuxing@xaut.edu.cn

Abstract: This study introduces a novel nonlinear dynamic analysis method, known as beluga whale optimization–slope entropy (BWO-SIEn), to address the challenge of recognizing sea state signals (SSSs) in complex marine environments. A method of underwater acoustic signal recognition based on BWO-SIEn and one-dimensional convolutional neural network (1D-CNN) is proposed. Firstly, particle swarm optimization–slope entropy (PSO-SIEn), BWO-SIEn, and Harris hawk optimization–slope entropy (HHO-SIEn) were used for feature extraction of noise signal and SSS. After 1D-CNN classification, BWO-SIEn were found to have the best recognition effect. Secondly, fuzzy entropy (FE), sample entropy (SE), permutation entropy (PE), and dispersion entropy (DE) were used to extract the signal features. After 1D-CNN classification, BWO-SIEn and 1D-CNN were found to have the highest recognition rate compared with them. Finally, compared with the other six recognition methods, the recognition rates of BWO-SIEn and 1D-CNN for the noise signal and SSS are at least 6% and 4.75% higher, respectively. Therefore, the BWO-SIEn and 1D-CNN recognition methods proposed in this paper are more effective in the application of SSS recognition.

Keywords: sea state signal; slope entropy; beluga whale optimization; one-dimensional convolutional neural network; feature extraction



Citation: Li, Y.; Gu, Z.; Fan, X.

Research on Sea State Signal

Recognition Based on Beluga Whale Optimization–Slope Entropy and One Dimensional–Convolutional Neural Network. *Sensors* **2024**, *24*, 1680.

<https://doi.org/10.3390/s24051680>

Academic Editor: Kah Phooi Seng

Received: 17 December 2023

Revised: 18 February 2024

Accepted: 2 March 2024

Published: 5 March 2024



Copyright: © 2024 by the authors. Licensee MDPI, Basel, Switzerland. This article is an open access article distributed under the terms and conditions of the Creative Commons Attribution (CC BY) license (<https://creativecommons.org/licenses/by/4.0/>).

1. Introduction

The earth is abundant in marine resources. With the advancements in human productivity and technology, there is a growing interest in utilizing, developing, and protecting the ocean [1–4]. In underwater signal transmission, acoustic signals serve as the primary carriers of information. However, underwater acoustic signals frequently exhibit non-stationary and nonlinear characteristics. Therefore, the key challenge lies in extracting information from non-stationary nonlinear signals [5,6]. Most traditional methods for extracting features from underwater acoustic signals involve converting the signals from the time domain to the frequency domain and extracting the spectral features. Short-time Fourier transform and Wigner–Ville distribution fail to adequately capture the relationship between signal frequency and time. Despite its ability to provide time–frequency information, the wavelet transform is limited by the choice of wavelet basis function [7,8]. While these methods have shown some success in practical applications, characterizing the nonlinearity of underwater acoustic signals remains challenging. Consequently, the traditional signal-processing methods are limited in their ability to address the nonlinear characteristics of underwater acoustic signals. Thus, there is a need to propose a new method for characterizing these nonlinear characteristics.

With the advancement of nonlinear science theory, fractal dimension (FD) has been proposed, but the traditional FD cannot represent the complexity information of multi-channel time series. Therefore, Yuxing Li et al. [9] proposed multivariate multiscale HFD

(MvmHFD). And the concept of information entropy, which quantifies the complexity and randomness of signals, has been introduced. Entropy measures such as approximate entropy (AE) [10,11], SE [12,13], FE [14,15], PE [16,17], and DE [18,19] have found extensive applications in the field of underwater acoustic signal recognition. The scope of entropy measurement methods has expanded over time, giving rise to various types. For instance, Costa proposed multiscale entropy (MSE) [20,21], which assesses the complexity of time series across different scales. Building upon MSE, Jinde Zheng et al. introduced multiscale permutation entropy (MPE) [22,23], multiscale fuzzy entropy (MFE) [24,25], and adaptive multiscale dispersion entropy (AMDE) [26,27]. Based on SE and MSE, Keheng Zhu et al. presented a hierarchical entropy (HE) method [28]. This approach involves hierarchical data decomposition, using sample entropy at each decomposition node to construct feature vectors, which are then used for fault identification through support vector machine techniques. Yongbo Li et al. proposed hierarchical fuzzy entropy (HFE) [29], a hierarchical analysis combined with fuzzy entropy calculation. Unlike MFE, HFE analyzes both low-frequency and high-frequency signal components, enabling more comprehensive and accurate information extraction. Yuxing Li et al. [30] developed a variable-step multiscale KFD (VSMKFD) to extract ship radiated noise features.

In 2019, David CuestaFra proposed a novel time series complexity estimator known as slope entropy (SIE) [31,32]. Due to its significant impact on classification, SIE has been widely used in various fields. Its effectiveness has been verified in disciplines such as medicine, hydroacoustics, and fault diagnosis. For example, Dakappa Pradeepa H et al. [33] conducted a time series analysis of fever using SIE, while CuestaFra David et al. [34] applied SIE to classify activity records of bipolar disorder patients. In the field of underwater acoustic signal recognition, SIE offers a comprehensive representation of the nonlinear characteristics of underwater acoustic signals, surpassing conventional entropy methods like Apen and SE. Furthermore, as SIE incorporates two threshold parameters that influence its performance [35,36], Li Yuxing et al. [37] proposed the PSO-SIE algorithm, which employs an optimization algorithm to determine these parameters. In the context of PSO, Li Wei et al. [38] introduced the concept of quantum behavior and proposed a variant called quantum-behaved particle swarm optimization (QPSO). The effectiveness of PSO was further demonstrated by Gao Yonglin et al. [39] in improving the performance of the LS-SVM model. This paper presents the BWO-SIE algorithm for feature extraction in underwater acoustic signals.

With the development of machine-learning algorithms, we can classify the features of the extracted signals through 1D-CNN [40,41], and the effective features can be automatically learned through training, thus achieving better classification results. Therefore, the recognition method of BWO-SIE and 1D-CNN is proposed in this paper and applied to underwater acoustic signal recognition.

The structure of this paper is divided into the following parts. Section 2 detail the algorithmic principle and steps of the proposed method, respectively. Sections 3 and 4 demonstrate the recognition experiments and analysis of noises and SSS, respectively. Finally, in Section 5, the innovation and experimental conclusions of this paper are discussed.

2. Algorithms

2.1. Slope Entropy

SIE is a complexity estimator for time series data that quantifies the complexity of a signal. It is a nonlinear dynamic indicator calculated solely based on the magnitude and five moments of the time series. A higher value of SIE indicates a more complex signal, while a lower value suggests a simpler signal. The complete calculation procedure for SIE is provided below:

Step 1: For a given time series, $D = \{d_i, i = 1, 2, 3, \dots, n\}$, where n indicates the number of elements in a time series. Then, set the embedding dimension, m . The time

series, D , can be divided into $k = n - m + 1$ subseries. The decomposition form of the time series, D , is as follows:

$$D_1 = \{d_1, d_2, \dots, d_m\}, D_2 = \{d_2, d_3, \dots, d_{m+1}\}, \dots, D_k = \{d_k, d_{k+1}, \dots, d_n\} \quad (1)$$

Step 2: For all subsequences obtained in (1), subtract the former from the latter of the two adjacent elements to obtain k new sequences:

$$T_1(i = 1, 2, \dots, k) = \{t_k, t_{k+1}, \dots, t_{n-1}\} \quad (2)$$

Each of the k new sequences in (2) contains $m - 1$ elements, which are $t_k = d_{k+1} - d_k$.

Step 3: Introduce the two SlEn threshold parameters, γ and δ . Here, $0 < \delta < \gamma$. Using the threshold parameters $-\gamma$, $-\delta$, δ , and γ as the dividing line, the numeric field is divided into five modules, namely -2 , -1 , 0 , 1 , and 2 , and all elements in the sequence obtained from Step 2 are compared to these two thresholds. If $t_k < -\gamma$, it is divided into module -2 . If $-\gamma < t_k < -\delta$, it is divided into module -1 . If $|t_k| < \delta$, it is divided into module 0 . If $\delta < t_k < \gamma$, it is divided into module 1 . If $t_k > \gamma$, it is divided into module 2 . The principle of module division is shown in Figure 1:

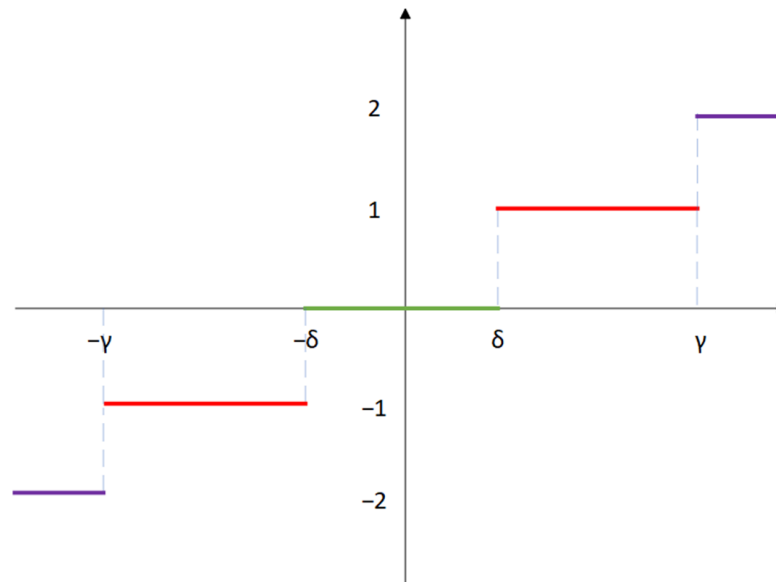


Figure 1. The principle of module division.

The partition sequence form is as follows:

$$E_k = \{e_k, e_{k+1}, \dots, e_{n-1}\} \quad (3)$$

Each element of E_k in (3) is one of the five modules, -2 , -1 , 0 , 1 , and 2 .

Step 4: Since there are five modules, there are, at most, $j = 5^{m-1}$ types of sequence E_k . For example, when m is 3, there are, at most, 25 types of E_k . These are {2,2}, {2,1}, {2,0}, {2,-1}, {2,-2}, ..., {-2,-1}, and {-2,-2}; the number of each type is recorded as r_1, r_2, \dots, r_j , and the frequency of each type is calculated as follows:

$$R_j = \frac{r_j}{k} \quad (4)$$

Step 5: Based on the classical Shannon entropy, the formula of SIE_n is defined as follows:

$$\text{SlopeEn}(m, \delta, \gamma) = - \sum_j R_j \ln R_j \quad (5)$$

where R_j is obtained from (4).

2.2. Beluga Whale Optimization

The BWO [42] algorithm is an optimization based on the bionics idea, which simulates the predation and mating behavior of the beluga whale population. It can be utilized for function optimization, machine learning, and neural networks. The following are the complete steps of the BWO algorithm:

- (1) First, an appropriate optimization problem is selected and transformed into a mathematical model. The determination of whether the target necessitates a minimum or maximum value, as well as the identification of the optimization variables, is required.
- (2) Initializing the beluga population. Specifically, beluga whale individuals are randomly generated, each containing optimization variables, which can be represented by a d-dimensional vector.
- (3) The fitness value of each individual beluga is calculated. Specifically, the optimization variable of each individual is substituted into the objective function to obtain the corresponding fitness value.
- (4) The beluga population members are ranked based on their fitness values. Specifically, the individual beluga whale with the highest fitness value is referred to as the “leader” individual.
- (5) The positions and speeds of the remaining beluga whales are updated based on the position and speed information of the leader.
- (6) The fitness value of the updated beluga whale population is recalculated, while the global historical optimal solution is updated.
- (7) Determine whether the maximum number of iterations has been reached. If it is satisfied, the optimal solution is generated, and the algorithm ends. Otherwise, go back to Step 4 and continue the iteration.

2.3. Beluga Whale Optimization–Slope Entropy

BWO-SIE_n is an improvement of SIE_n, and its basic idea is to optimize the two threshold parameters of an SIE_n through an optimization algorithm. According to this idea, the signal recognition methods of BWO-SIE_n and 1D-CNN are proposed in this paper. The basic steps are as follows:

Step 1: The average recognition rate of 1D-CNN recognition signals is taken as the objective function, and the two independent variables of the function are δ , and γ .

Step 2: Algorithm initialization. Set the population quantity as “noop” and the maximum number of iterations as “ T_{\max} ”. Seek the values of δ and γ corresponding to the maximum average recognition rate.

Step 3: Calculate the fitness (average recognition rate) of each individual, find the individual with the highest fitness, and designate it as the “leader” individual.

Step 4: According to the position and speed information of the leader, the BWO algorithm is used to update the position and speed of other individuals.

Step 5: If the maximum number of iterations, T_{\max} , has not been reached, iterate once more from Step 3 in order to identify the individual displaying the highest level of fitness.

Step 6: After reaching the maximum number of iterations, T_{\max} , output the iteration time and the two parameter values represented by the individual with the highest fitness.

The flow of the BWO-SIE_n algorithm is shown in Figure 2.

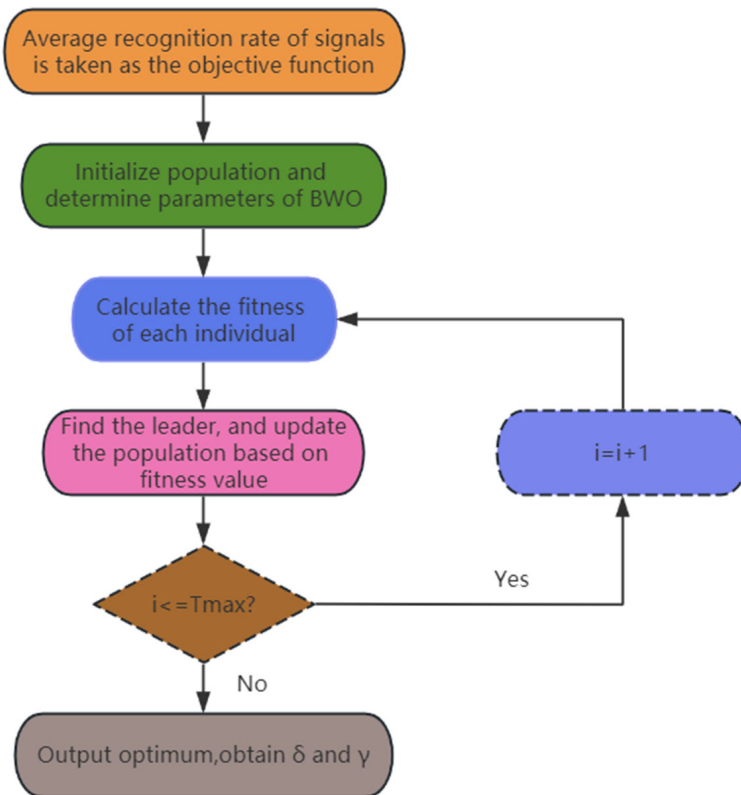


Figure 2. The flow of BWO-SIEn algorithm.

2.4. One Dimensional Convolutional Neural Network

A 1D-CNN [43] is a variant of the convolutional neural network. The 1D-CNN is mainly used to process one-dimensional sequence data. Compared with traditional fully connected neural networks, the 1D-CNN can better deal with local relationships in sequence data. The network structure used in this study is shown in Figure 3.

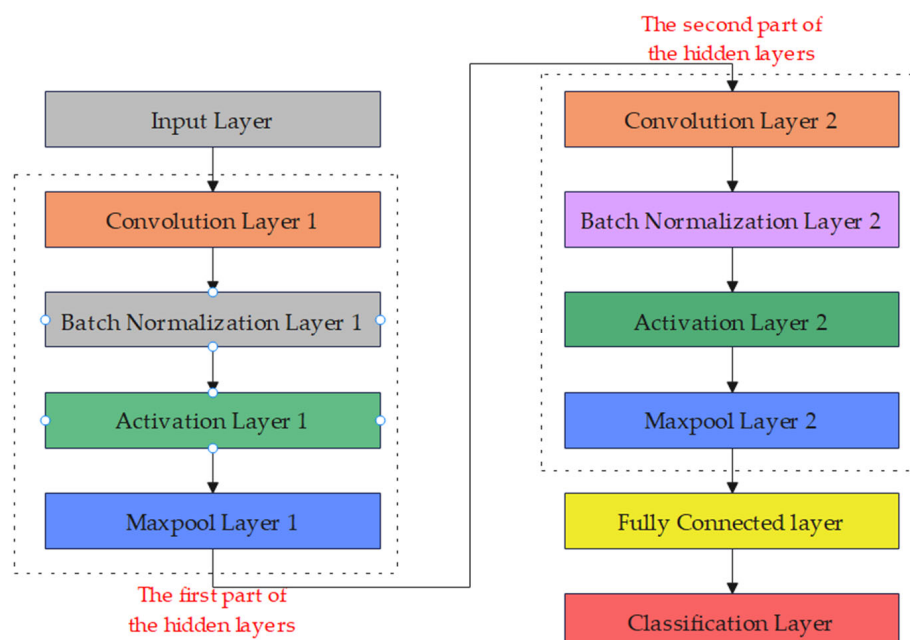


Figure 3. The 1D-CNN model structure.

The dimension of the input data for the input layer is 15. The first part of the hidden layer is configured as follows: The convolutional layer consists of 64 convolutional kernels with a size of 2. The batch normalization layer performs batch normalization on the output of convolutional layer. The activation layer applies the rectified linear unit (ReLU) function to activate the output of the convolutional layer. The window size of the max pooling layer in the time dimension is 2, with a stride of 1. The second part of the hidden layer is much the same as the first, except convolutional layer 2 contains 32 convolutional kernels with a size of 2. The output size of the fully connected layer is 4, corresponding to 4 categories. The classification layer performs classification on the output and obtains the final prediction result.

The training parameters and configuration of the neural network are summarized as follows: the network parameters are updated by using the Adam gradient descent algorithm; a maximum of 500 epochs are conducted; the initial learning rate is set to 0.0001; L2 regularization parameter of 0.0001 is applied; the learning rate is decreased using a piecewise linear decay strategy, with the learning rate reduced to 0.1 times its original value after every 450 epochs; and before each epoch, the training set samples are shuffled.

2.5. The Recognition Method Based on Beluga Whale Optimization–Slope Entropy and One-Dimensional Convolutional Neural Network

Combining BWO-SIEn and 1D-CNN, a new SSS recognition method is proposed, BWO-SIEn is used for feature extraction, and 1D-CNN is used to classify the extracted features. The specific steps of the proposed method are as follows:

Step 1: The SSSs are divided into signal samples for feature extraction. In this paper, four types of SSSs are divided into samples, and each SSS type has 3000 signal samples, with each sample containing 4096 data points.

Step 2: The signal samples of the SSSs are calculated by BWO-SIEn. In this paper, four types of SSS signal samples are calculated, each type of SSS to obtain 3000 feature samples, a total of 12,000 feature samples.

Step 3: The feature samples are input into the neural network for classification. In this paper, the 3000 feature samples of each type of SSS are reset to a 200×15 matrix and then input to 1D-CNN.

3. Noise Signal Classification and Recognition Based on Beluga Whale Optimization–Slope Entropy and One-Dimensional Convolutional Neural Network

3.1. Introduction to Noise Signal

The simulation signal uses four different noise signals, namely blue noise, red noise, pink noise, and violet noise. Blue noise can produce higher energy at higher frequencies, and its power density is proportional to frequency. Red noise can produce a lot of energy at low frequencies, and its power density is inversely proportional to each octave. The power spectral density of pink noise is inversely proportional to each octave, and the intensity of each octave is equal. Violet noise produces very high energy at higher frequencies, and its power density is proportional to each octave. The data length of each noise signal used in the experiment in this section is 16,384,000. Noise signal waveforms in the time and frequency domains are shown in Figure 4.

It can be seen from Figure 4 that, in the frequency domain, blue noise and violet noise are similar, and their power density is proportional to frequency. Red noise is similar to pink noise, and its power density is inversely proportional to frequency.

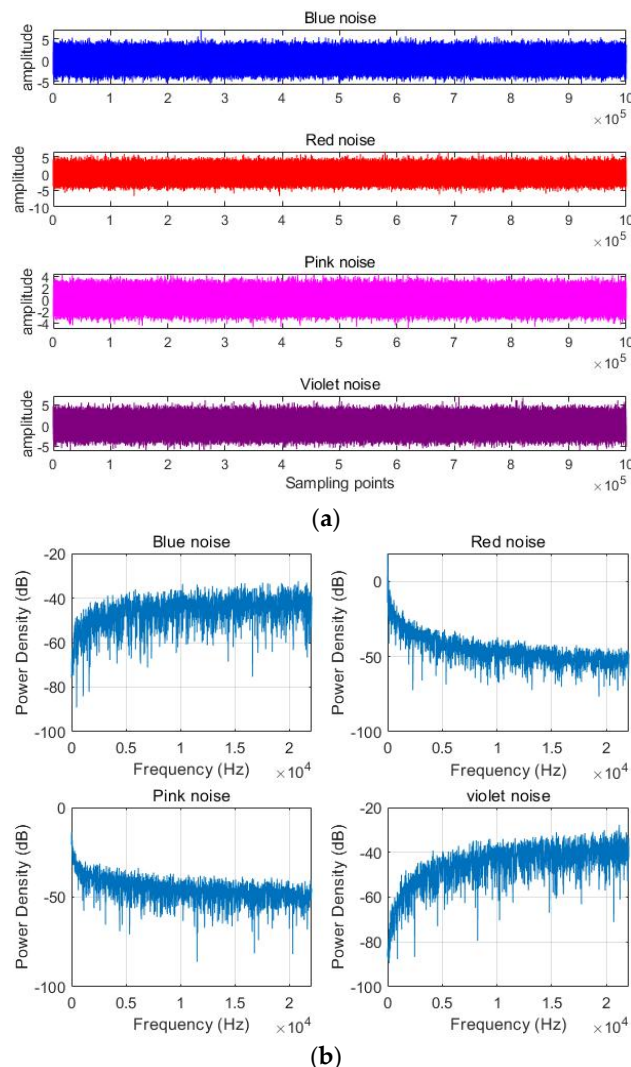


Figure 4. Noise signal waveforms in (a) time domain and (b) frequency domain.

3.2. Slope Entropy Optimization

For the purpose of comparison, identical parameters are set for all three optimization algorithms. The parameter settings for these algorithms are presented in Table 1.

Table 1. Parameter settings for different optimization algorithms.

Optimization Algorithms	Parameter Setting	
	Initial Population	Number of Iterations
PSO	10	30
BWO	10	30
HHO	10	30

The three optimization algorithms undergo 30 iterations. In each iteration, the SIE_n of all individuals in the population is computed, and then classification is performed using 1D-CNN. The objective function is set as the maximum recognition rate of the noise signal. The iteration time and the average recognition rate of the noise signal are then recorded. The optimization results of the three optimization algorithms are shown in Table 2.

Table 2. The optimization results of the three optimization algorithms.

Optimization Algorithm	Optimization Result			
	γ	δ	Optimization Time (s)	Recognition Rate (%)
PSO	0.4278	0.0001	81,231.45	75.25
BWO	0.2841	0.0495	121,458.37	82.75
HHO	0.1169	0.0166	168,911.81	76.75

Table 2 shows that, among the three optimization algorithms for optimizing SIEEn, PSO-SIEEn has the shortest optimization time but the lowest noise signal recognition rate. HHO-SIEEn has the longest optimization time but a moderate recognition rate. However, BWO-SIEEn has an intermediate optimization time and the highest recognition rate. Therefore, among the three optimization methods, the feature extraction method of BWO-SIEEn is the most effective for recognizing noise signals.

3.3. Based on Different Feature Extraction and One-Dimensional Convolutional Neural Network

To demonstrate the effectiveness of the BWO-SIEEn and 1D-CNN methods in noise signal recognition, seven signal recognition methods are compared in this experiment, including the unoptimized SE, FE, PE, DE, and 1D-CNN recognition methods, as well as the three optimized SIEEn and 1D-CNN methods proposed in Section 3.2. The parameter settings for the unoptimized entropy method can be found in Table 3.

Table 3. The parameter settings for the unoptimized entropy method.

Entropy Methods	Optimization Result			
	Embedding Dimension (m)	Threshold (r)	Number of Classes (nc)	Delay Time (tau)
SE	2	0.15	-	1
FE	2	0.15	-	1
PE	4	-	-	1
DE	4	-	6	1

Starting from the first data point of the signal, the generated noise signal is sampled, with every 4096 data points being taken as a signal sample. A total of 3000 signal samples are obtained for each type of noise. The 3000 noise signal samples are calculated by using the entropy value to obtain 3000 entropy samples. Every 15 entropy samples are served as one neural network sample, resulting in 200 neural network samples for each type of noise. The neural network samples for each type of noise are divided into 100 samples for the test set and the remaining 100 samples for the training set.

Multiple entropy methods are employed to extract the complexity features from four types of noise. The dimensionality of the entropy sample's feature points is 15. To facilitate visualization, T-Distributed Stochastic Neighbor Embedding (T-SNE) is utilized for reducing their dimensionality to a two-dimensional space. T-SNE map maps high-dimensional features to a two-dimensional space, with the horizontal and vertical coordinates being the two dimensions of the mapping, without any actual coordinates or meanings.

In the two-dimensional descending scatter diagram of the output layer features of the T-SNE test set, different colors represent different signals. The relationship between signals in different feature extraction can be visually observed by the degree of aggregation of dimensionality reduction points. The denser the points of the same color are and the further away they are from other points of the same color, the more it indicates that the signal is recognized correctly after such feature extraction. If several different points gather together more, it can show that these signals are not easy to distinguish between each other after this feature extraction. The two-dimensional descending scatter diagram of the output layer features of the T-SNE test set based on different features is shown in Figure 5.

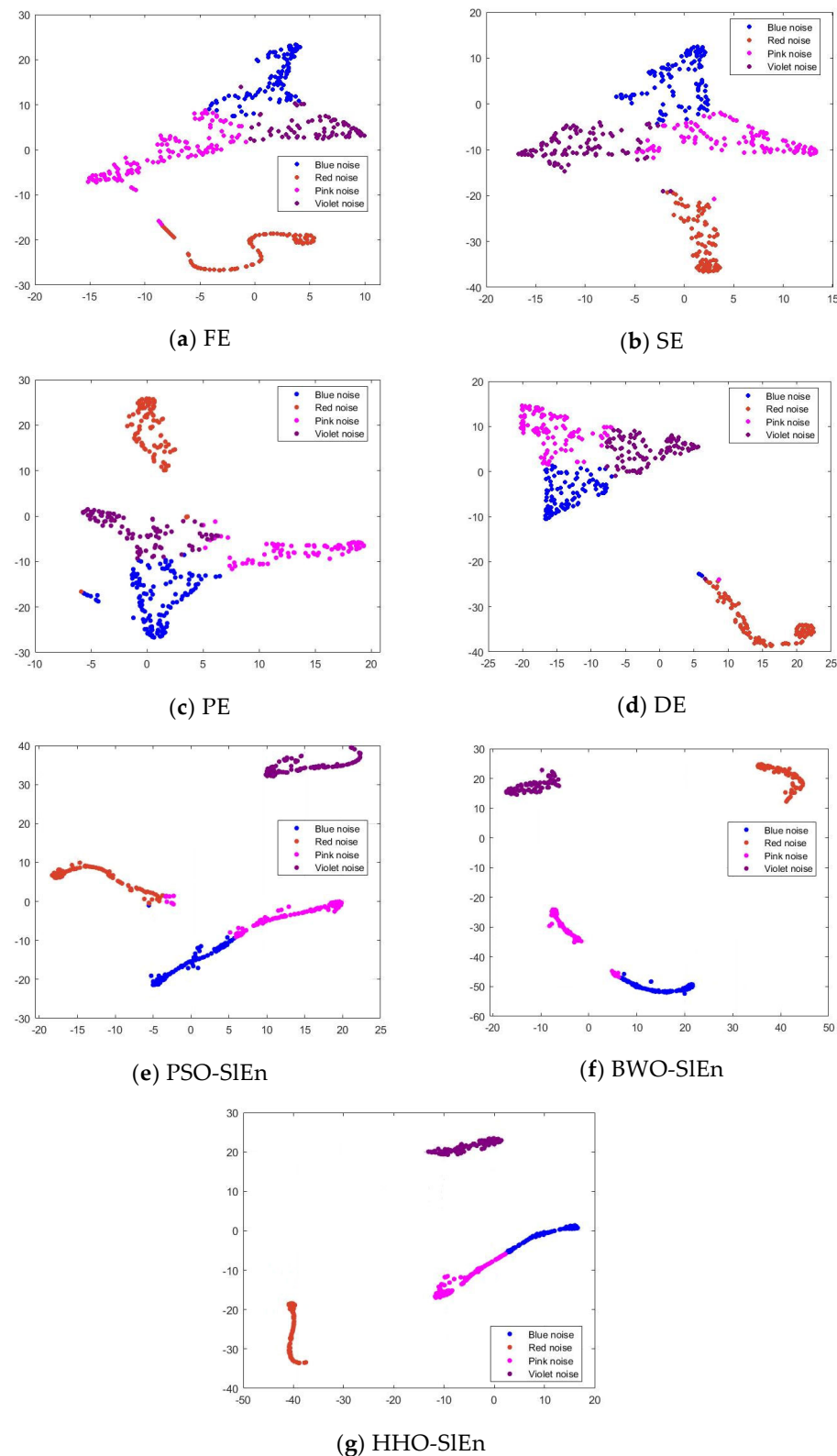


Figure 5. Two-dimensional scatterplot of output layer features of T-SNE test set based on different features.

To demonstrate the effectiveness of BWO-SIEn, this study calculates the number of correctly recognized signals in each signal class and the overall signal recognition rate for each recognition method. The confusion matrix can quantify the classification situation of

the signal through 1D-CNN based on the numbers after signal classification. Compared to Figure 5, it is much clearer to see the correct recognition rate for each signal.

The confusion matrix obtained after signal feature classification clearly shows the specific recognition situation of each type of signal, as shown in Figure 6. The recognition rate calculations are presented in Table 4 and are based on various feature extraction and 1D-CNN recognition methods for noise signal identification.

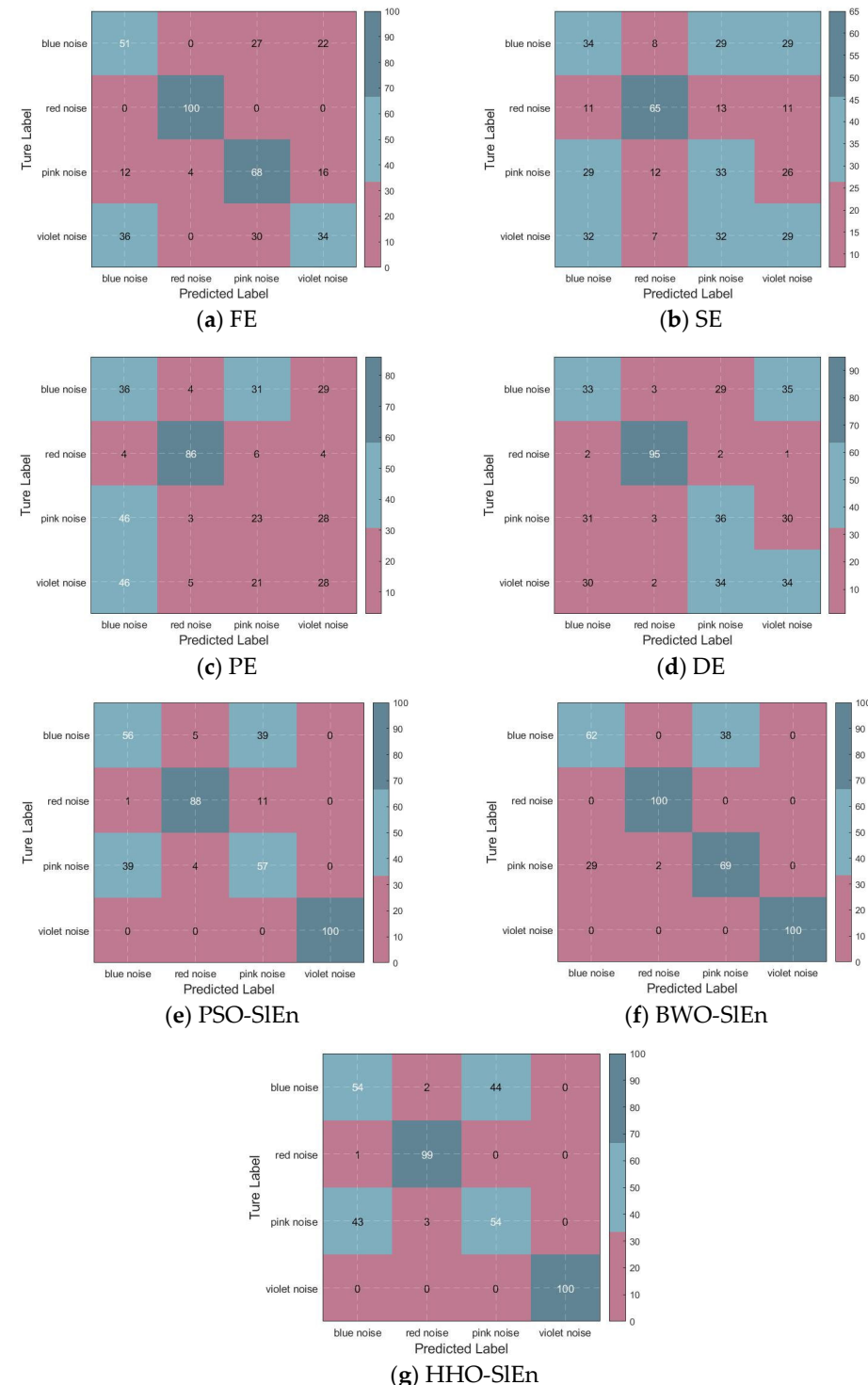


Figure 6. Confusion matrix for signal recognition.

Table 4. Four types of noise recognition results.

Feature Extraction	Number of Samples Correctly Identified				Average Recognition Rates (%)
	Blue Noise	Red Noise	Pink Noise	Violet Noise	
FE	51	100	68	34	63.25
SE	34	65	33	29	40.25
PE	36	86	23	28	43.25
DE	33	95	36	34	49.50
PSO-SIEn	56	88	57	100	75.25
BWO-SIEn	62	100	69	100	82.75
HHO-SIEn	54	99	54	100	76.75

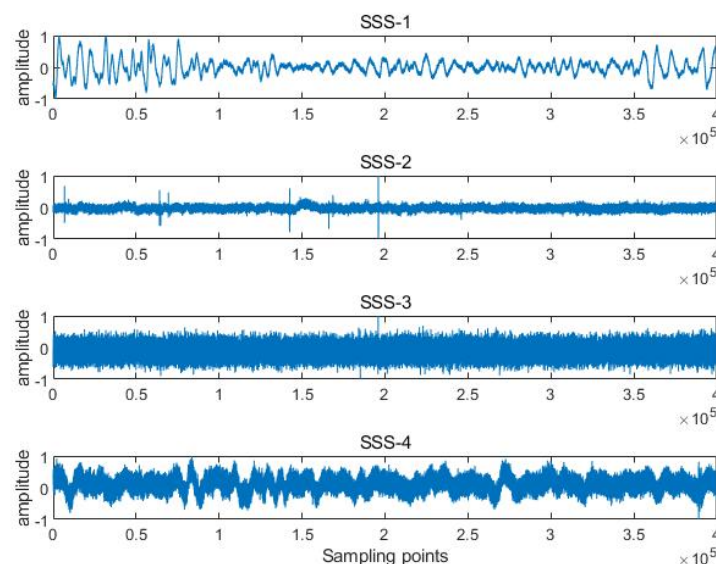
According to Figure 6 and Table 4, the recognition methods using FE and BWO-SIEn can completely identify the red noise; the three recognition methods using optimized SIEn can entirely identify the violet noise; the correct identification number of blue noise and pink noise for all recognition methods is below 70; the recognition rates of the recognition methods using optimized SIEn are higher than those of the unoptimized SIEn; among these three recognition methods using optimized SIEn, the recognition rates of BWO-SIEn are higher than others.

The experimental results demonstrate that the recognition methods using optimized SIEn have more effective recognition than unoptimized SIEn; among these three recognition methods using optimized SIEn, BWO-SIEn exhibits a better recognition ability than others. These demonstrate the necessity of optimizing SIEn parameters, the superiority of BWO global search, and the effectiveness of the method proposed in this paper for the accurate recognition of signals with nonlinear and non-stationary characteristics.

4. Experiments and Results

4.1. Introduction of Sea State Signal

Feature extraction is implemented for four types of measured SSSs, termed SSS-1, SSS-2, SSS-3, and SSS-4. Four types of SSSs derive from the same website [44]. The SSSs were collected from the Glacier Bay in Alaska, USA. SSS-1 represents light wind on the sea surface. SSS-2 represents snowfall on the sea surface. SSS-3 represents wind and ship noise. SSS-4 represents heavy rain on the sea surface. The sound of them was recorded by an underwater hydrophone. The length of the sampling point for SSS-1, SSS-2, and SSS-4 is 1,379,568, and the sampling length for SSS-3 is 1,313,904. The sampling frequency of them is 44,100 hz. SSS waveforms in the time domain are shown in Figure 7.

**Figure 7.** SSS waveforms in time domain.

By studying and recognizing these signals, researchers can gain insights into the prevailing weather patterns, oceanic processes, and their impacts on marine ecosystems. This knowledge is crucial for maritime navigation, weather forecasting, climate studies, and marine resource management. It allows for the development of effective strategies to mitigate the adverse effects of these oceanic conditions on human activities and to promote safety and sustainability in marine environments.

4.2. Based on Different Feature Extraction and One-Dimensional Convolutional Neural Network

To demonstrate that the recognition effectiveness of SSS based on the BWO-SIEn and 1D-CNN method is the best, the experimental design steps for SSS are the same as those for noise signals. At the same time, the parameter settings for the optimization algorithms remain consistent with Table 1, and the parameter settings for the unoptimized entropy methods remain consistent with Table 3. The results of optimizing the SIEn using the three optimization algorithms for the SSS experiment are shown in Table 5.

Table 5. The results of SIEn optimization by different optimization algorithms.

Optimization Algorithm	Optimization Result			
	γ	δ	Optimization Time (s)	Recognition Rate (%)
PSO	0.83294	0.007075	109,758.06	87.75
BWO	0.4219	0.0283	264,082.98	92.50
HHO	0.1024	0.0226	296,172.29	85.75

As illustrated in Table 5, among the three optimization algorithms, the optimization time of HHO-SIEn is the longest, and the recognition rate of SSS is the lowest. PSO-SIEn has the shortest optimization time, but the recognition rate of sea is lower than that of BWO-SIEn. The optimization time of BWO-SIEn is moderate, and the recognition rate of SSS is the highest. Therefore, among the three optimization methods, the feature extraction method of BWO-SIEn is the most effective for SSS recognition.

Due to the limited length of the data of the SSS, in order to ensure the number of data points in the signal sample, when taking the data points of 3000 samples of the SSS sample, the starting point of the signal sample is randomly taken from the original signal, and then 4096 data points are taken backward. The starting point of SSS-1, SSS-2, and SSS-4 is set to the range of [1, 1,375,472], and the sample starting point of SSS-3 is set to the range of [1, 1,309,808]. A sample matrix of 3000×4096 is obtained for each SSS. The partition of the remaining entropy samples and neural samples is completely consistent with the simulation experimental signal. In order to facilitate observation, the dimension of the noise complexity feature points is reduced to two-dimensional space by T-SNE. The two-dimensional reduced-order scatter plot of the output layer features of the T-SNE test set based on different features is shown in Figure 8.

After performing a 1D-CNN classification on the four types of SSS features, the following information can be obtained from Figure 7. Among the recognition methods using unoptimized SIEn, PE only distinguishes SSS-3 well; DE has poor distinguishability for SSS-1 and SSS-2, as well as for SSS-3 and SSS-4; FE and SE exhibit low distinguishability for SSS-3 and SSS-4 but high distinguishability for the other two types of noise. Among the recognition methods using optimized SIEn, they show high distinguishability for SSS-1 and SSS-4, but PSO-SIEn and HHO-SIEn have lower distinguishability for SSS-2 and SSS-3 compared to BWO-SIEn.

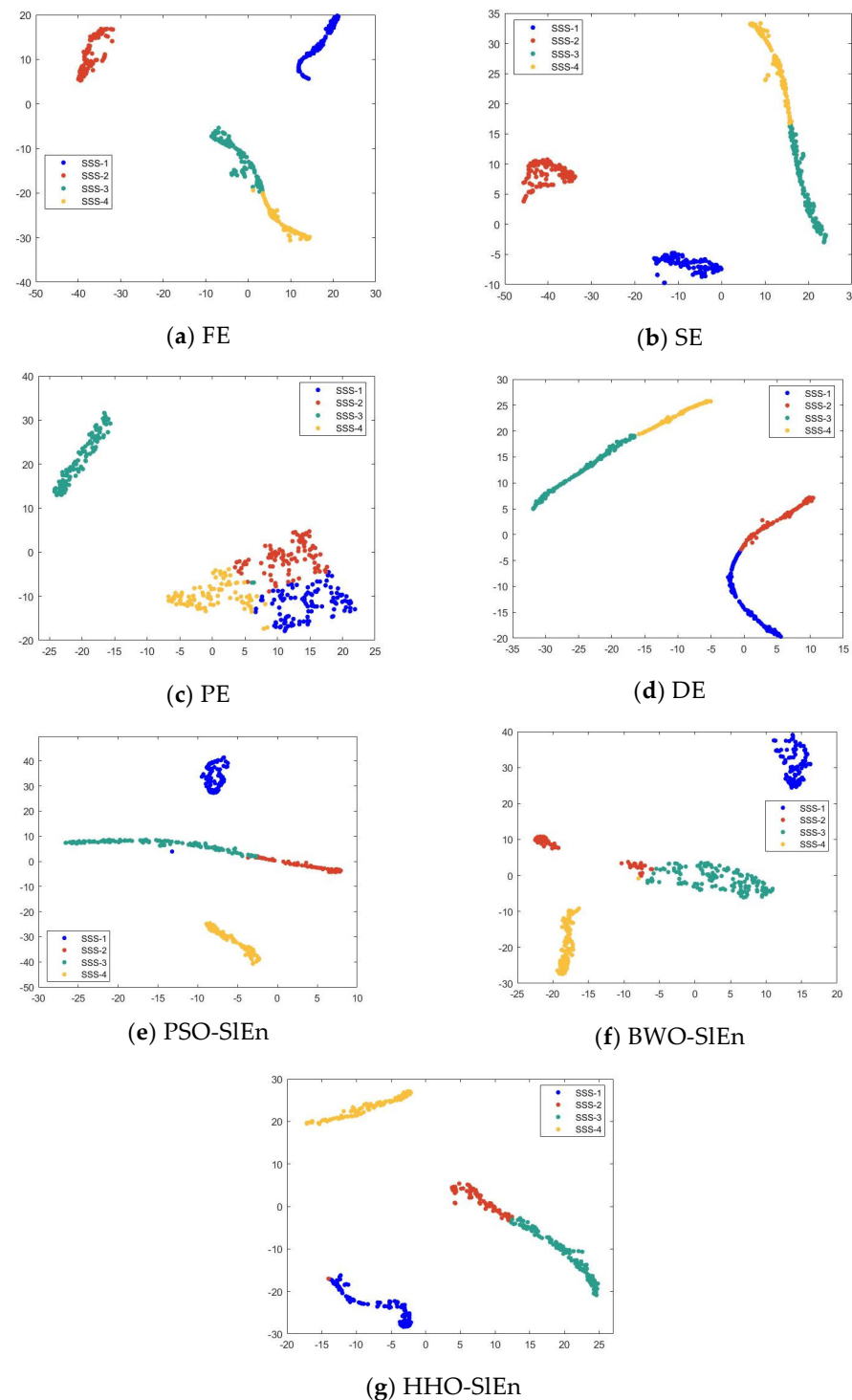


Figure 8. Two-dimensional scatterplot of output layer features of T-SNE test set based on different features.

To demonstrate the effectiveness of BWO-SIEn, this study calculates the number of correctly recognized signals in each signal class and the overall signal recognition rate for each recognition method. The confusion matrix obtained after signal feature classification clearly shows the specific recognition situation of each type of signal, as shown in Figure 9. The recognition rate calculations are presented in Table 6 and are based on various feature extraction and 1D-CNN recognition methods for noise signal identification.

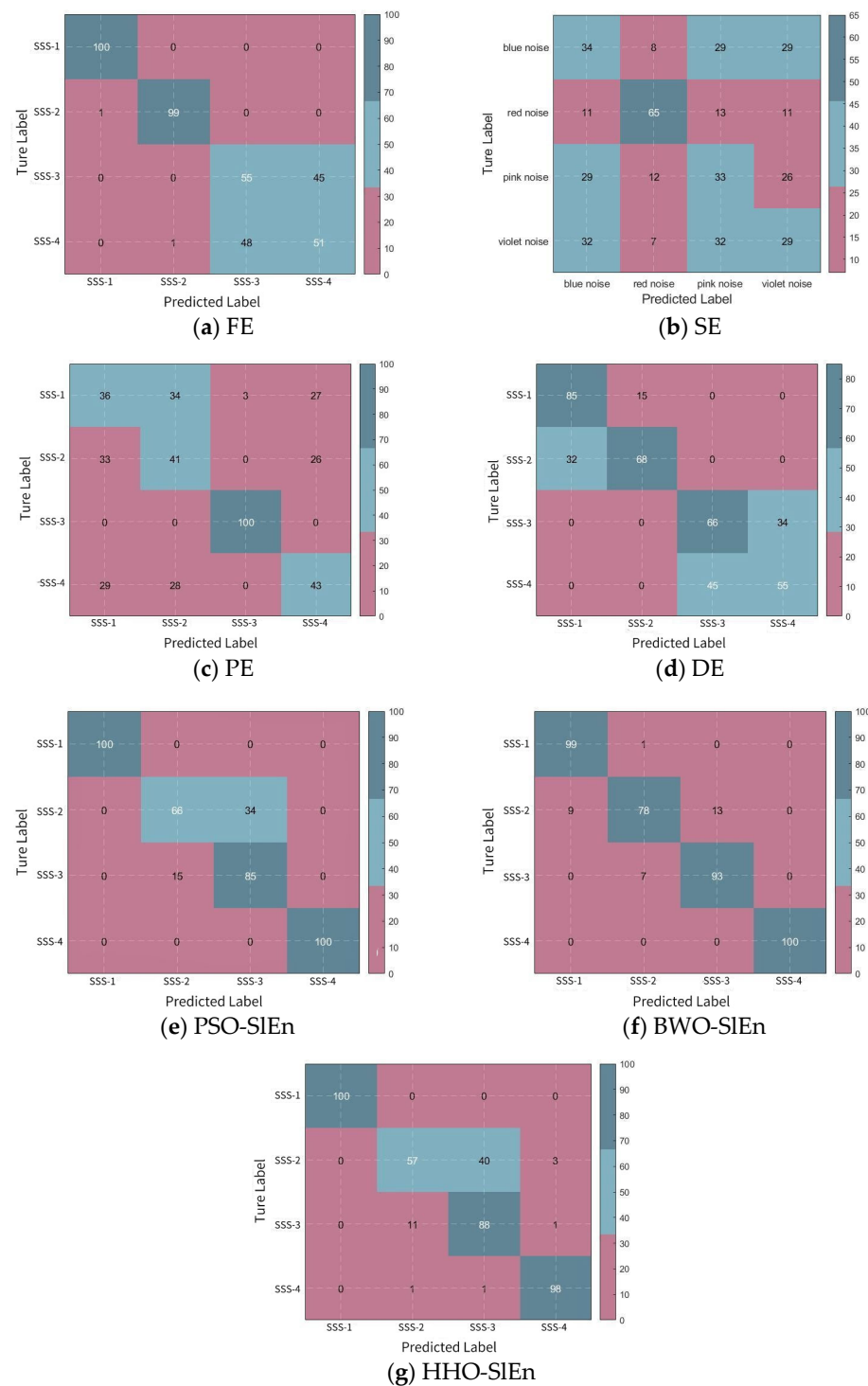


Figure 9. Confusion matrix for signal recognition.

As illustrated in Figure 9 and Table 6, the recognition methods using FE can recognize SSS-1 and SSS-2 above 99; the recognition methods using PE can completely identify SSS-3; the recognition methods that optimized SIEn can identify SSS-1 and SSS-4 above 98, and the recognition rates of them are higher than those of unoptimized SIEn; among the three recognition methods using optimized SIEn, only BWO-SIEn identified all four types of SSS above 75, and the recognition rate of BWO-SIEn is higher than others.

Table 6. Four types of sea state signal-recognition results.

Feature Extraction	Number of Samples Correctly Identified				Average Recognition Rates (%)
	SSS-1	SSS-2	SSS-3	SSS-4	
FE	100	99	55	51	76.25
SE	100	100	63	45	77.00
PE	36	41	100	43	55.00
DE	85	68	66	55	68.50
PSO-SIEn	100	66	85	100	87.75
BWO-SIEn	99	78	93	100	92.50
HHO-SIEn	100	57	88	98	85.75

The experimental results demonstrate that the recognition methods using optimized SIEn have more effective recognition than unoptimized SIEn; among these three recognition methods using optimized SIEn, BWO-SIEn exhibits better recognition ability than others. This demonstrates that optimizing SIEn parameters is necessary; BWO possesses stronger global search capabilities in contrast to PSO and HHO, and the method proposed in this paper is effective for accurate recognition of SSS with nonlinear and non-stationary characteristics. This finding is in accordance with the results of our noise experiment.

5. Conclusions

Based on the theory of SIEn, the optimized SIEn is proposed and applied to the feature extraction of SSS, and then an SSS recognition method based on BWO-SIEn and 1D-CNN is proposed. The feasibility of the proposed method is verified through the experiment of classification and recognition of four types of noise signals and four types of SSS. The main innovation points and conclusions of this study are as follows:

- (1) BWO was used to optimize SIEn for the first time, and this method was used to extract the features of SSS. Then, 1D-CNN was used as the classifier, and the signal recognition method of BWO-SIEn and 1D-CNN was proposed.
- (2) Compared to the PSO-SIEn and HHO-SIEn methods, the BWO-SIEn and 1D-CNN method achieved at least 6% and 4.75% higher average recognition rates for noise signals and sea condition signals.
- (3) The recognition rates of the proposed BWO-SIEn were 24.7% and 17.5% higher than the average recognition rates of the other six recognition methods in noise signal and SSS, respectively.

Author Contributions: Y.L., methodology, software, writing—original draft, and funding acquisition; Z.G., methodology, software, data curation, and writing—original draft; X.F., writing—review and editing, visualization, and supervision. All authors have read and agreed to the published version of the manuscript.

Funding: This research was funded by the Natural Science Foundation of Shaanxi Province (grant no. 2022JM-337).

Institutional Review Board Statement: Not applicable.

Informed Consent Statement: Not applicable.

Data Availability Statement: The datasets analyzed during the current study are available from the corresponding author upon reasonable request.

Conflicts of Interest: The authors declare no conflict of interest.

Nomenclature

FE	fuzzy entropy
SE	sample entropy
PE	permutation entropy
DE	dispersion entropy
AE	approximate entropy
MSE	multiscale entropy
MPE	multiscale permutation entropy
MFE	multiscale fuzzy entropy
made	adaptive multiscale dispersion entropy
HE	hierarchical entropy
HFE	hierarchical fuzzy entropy
T-SNE	T-Distributed Stochastic Neighbor Embedding
SSS	sea state signal
MvmHFD	multivariate multiscale HFD
QPSO	quantum-behaved particle swarm optimization
PSO	particle swarm optimization
BWO	beluga whale optimization
HHO	Harris hawk optimization
SIE	slope entropy
1D-CNN	one-dimensional convolutional neural network

References

- Xu, K.; Xu, Q.; You, K.; Zhu, B.; Feng, M.; Feng, D.; Liu, B. Self-supervised learning-based underwater acoustical signal classification via mask modeling. *J. Acoust. Soc. Am.* **2023**, *154*, 5–15. [[CrossRef](#)] [[PubMed](#)]
- Zhang, Y.; Zeng, Q. MSLEFC: A low-frequency focused underwater acoustic signal classification and analysis system. *Eng. Appl. Artif. Intell.* **2023**, *123*, 10633. [[CrossRef](#)]
- Zhu, Z.; Ma, S.; Zhu, X.; Lan, Q.; Piao, S.; Cheng, Y. Parallel optimization of underwater acoustic models: A survey. *Chin. Phys. B* **2022**, *31*, 104301. [[CrossRef](#)]
- Zhou, F.; Fan, J.; Wang, B.; Zhou, Y.; Huang, J. Acoustic barcode based on the acoustic scattering characteristics of underwater targets. *Appl. Acoust.* **2022**, *189*, 108607. [[CrossRef](#)]
- Zhu, Q.; Alwan, A. Non-linear feature extraction for robust speech recognition in stationary and non-stationary noise. *Comput. Speech Lang.* **2003**, *17*, 381–402. [[CrossRef](#)]
- Li, Y.; Zhou, Y.; Jiao, S. Multi-scale ensemble dispersion Lempel-Ziv complexity and its application on feature extraction for ship-radiated noise. *Appl. Acoust.* **2024**, *218*, 109890. [[CrossRef](#)]
- Hu, Y.; Li, F.; Li, H.; Liu, C. An enhanced empirical wavelet transform for noisy and non-stationary signal processing. *Digit. Signal Process.* **2017**, *60*, 220–229. [[CrossRef](#)]
- Balubaid, M.; Sattari, M.A.; Taylan, O.; Bakhsh, A.A.; Nazemi, E. Applications of discrete wavelet transform for feature extraction to increase the accuracy of monitoring systems of liquid petroleum products. *Mathematics* **2021**, *9*, 3215. [[CrossRef](#)]
- Li, Y.; Zhang, S.; Liang, L.; Ding, Q. Multivariate Multiscale Higuchi Fractal Dimension and Its Application to Mechanical Signals. *Fractal Fract.* **2024**, *8*, 56. [[CrossRef](#)]
- Lahmiri, S.; Tadj, C.; Gargour, C.; Bekiros, S. Characterization of infant healthy and pathological cry signals in cepstrum domain based on approximate entropy and correlation dimension. *Chaos Solitons Fractals* **2021**, *143*, 110639. [[CrossRef](#)]
- Nicoletti, R.; Cavalini, A.A.; Steffen, V. Detection of cracks in rotating shafts by using the combination resonances approach and the approximated entropy algorithm. *J. Vib. Shock* **2018**, *2018*, 4094631. [[CrossRef](#)]
- Richman, J.S.; Moorman, J.R. Physiological time-series analysis using approximate entropy and sample entropy. *Am. J. Physiol.-Heart Circ. Physiol.* **2000**, *278*, H2039–H2049. [[CrossRef](#)] [[PubMed](#)]
- Tomčala, J. New fast ApEn and SampEn entropy algorithms implementation and their application to supercomputer power consumption. *Entropy* **2020**, *22*, 863. [[CrossRef](#)] [[PubMed](#)]
- Kosko, B. Fuzzy entropy and conditioning. *Inf. Sci.* **1986**, *40*, 165–174. [[CrossRef](#)]
- Qaid, M.S.A.; Basah, S.N.; Yazid, H.; Som, M.H.M.; Basaruddin, K.S.; Hassan, M.K.A. Performance analysis of diabetic retinopathy detection using fuzzy entropy multi-level thresholding. *Measurement* **2023**, *216*, 112887. [[CrossRef](#)]
- Bandt, C.; Pompe, B. Permutation entropy: A natural complexity measure for time series. *Phys. Rev. Lett.* **2002**, *88*, 174102. [[CrossRef](#)] [[PubMed](#)]
- Rajabi, S.; Azari, M.S.; Santini, S.; Flammini, F. Fault diagnosis in industrial rotating equipment based on permutation entropy, signal processing and multi-output neuro-fuzzy classifier. *Expert Syst. Appl.* **2022**, *206*, 117754. [[CrossRef](#)]

18. Rostaghi, M.; Azami, H. Dispersion entropy: A measure for time-series analysis. *IEEE Signal Process. Lett.* **2016**, *23*, 610–614. [[CrossRef](#)]
19. Li, Y.; Jiao, S.; Deng, S.; Geng, B.; Li, Y. Refined composite variable-step multiscale multimapping dispersion entropy: A nonlinear dynamical index. *Nonlinear Dyn.* **2024**, *112*, 2119–2137. [[CrossRef](#)]
20. Costa, M.; Goldberger, A.L.; Peng, C.-K. Multiscale entropy analysis of biological signals. *Phys. Rev. E* **2005**, *71*, 021906. [[CrossRef](#)]
21. Zheng, J.; Li, Y.; Zhai, Y.; Zhang, N.; Yu, H.; Tang, C.; Yan, Z.; Luo, E.; Xie, K. Effects of sampling rate on multiscale entropy of electroencephalogram time series. *Biocybern. Biomed. Eng.* **2023**, *43*, 233–245. [[CrossRef](#)]
22. Zheng, J.; Chen, Y.; Pan, H.; Tong, J. Composite multi-scale phase reverse permutation entropy and its application to fault diagnosis of rolling bearing. *Nonlinear Dyn.* **2023**, *111*, 459–479. [[CrossRef](#)]
23. Minhas, A.S.; Singh, S. A new bearing fault diagnosis approach combining sensitive statistical features with improved multiscale permutation entropy method. *Knowl.-Based Syst.* **2021**, *218*, 106883. [[CrossRef](#)]
24. Zheng, J.; Cheng, J.; Yang, Y.; Luo, S. A rolling bearing fault diagnosis method based on multi-scale fuzzy entropy and variable predictive model-based class discrimination. *Mech. Mach. Theory* **2014**, *78*, 187–200. [[CrossRef](#)]
25. Borin, A.M.S.; Silva, L.E.V.; Murta, L.O. Modified multiscale fuzzy entropy: A robust method for short-term physiologic signals. *Chaos Interdiscip. J. Nonlinear Sci.* **2020**, *30*, 083135. [[CrossRef](#)] [[PubMed](#)]
26. Li, C.; Zheng, J.; Pan, H.; Liu, Q. Fault diagnosis method of rolling bearings based on adaptive multi-scale dispersion entropy. *Noise Vib. Control* **2018**, *38*, 173–178.
27. Luo, S.; Yang, W.; Luo, Y. Fault diagnosis of a rolling bearing based on adaptive sparest narrow-band decomposition and RefinedComposite multiscale dispersion entropy. *Entropy* **2020**, *22*, 375. [[CrossRef](#)]
28. Zhu, K.; Song, X.; Xue, D. A roller bearing fault diagnosis method based on hierarchical entropy and support vector machine with particle swarm optimization algorithm. *Measurement* **2014**, *47*, 669–675. [[CrossRef](#)]
29. Li, Y.; Xu, M.; Zhao, H.; Huang, W. Hierarchical fuzzy entropy and improved support vector machine based binary tree approach for rolling bearing fault diagnosis. *Mech. Mach. Theory* **2016**, *98*, 114–132. [[CrossRef](#)]
30. Li, Y.; Zhou, Y.; Jiao, S. Variable-Step Multiscale Katz Fractal Dimension: A New Nonlinear Dynamic Metric for Ship-Radiated Noise Analysis. *Fractal Fract.* **2024**, *8*, 9. [[CrossRef](#)]
31. Cuesta-Frau, D. Slope entropy: A new time series complexity estimator based on both symbolic patterns and amplitude information. *Entropy* **2019**, *21*, 1167. [[CrossRef](#)]
32. Kouka, M.; Cuesta-Frau, D. Slope Entropy Characterisation: The Role of the δ Parameter. *Entropy* **2022**, *24*, 1456. [[CrossRef](#)] [[PubMed](#)]
33. Cuesta-Frau, D.; Dakappa, P.H.; Mahabala, C.; Gupta, A.R. Fever time series analysis using slope entropy. Application to early unobtrusive differential diagnosis. *Entropy* **2020**, *22*, 1034. [[CrossRef](#)] [[PubMed](#)]
34. Cuesta-Frau, D.; Schneider, J.; Bakštein, E.; Vostatek, P.; Spaniel, F.; Novák, D. Classification of actigraphy records from bipolar disorder patients using slope entropy: A feasibility study. *Entropy* **2020**, *22*, 1243. [[CrossRef](#)] [[PubMed](#)]
35. Li, Y.; Tang, B.; Jiao, S.; Su, Q. Snake Optimization-Based Variable-Step Multiscale Single Threshold Slope Entropy for Complexity Analysis of Signals. *IEEE Trans. Instrum. Meas.* **2023**, *72*, 6505313. [[CrossRef](#)]
36. Li, Y.; Tang, B.; Jiao, S.; Zhou, Y. Optimized multivariate multiscale slope entropy for nonlinear dynamic analysis of mechanical signals. *Chaos Solitons Fractals* **2024**, *179*, 114436. [[CrossRef](#)]
37. Li, Y.; Mu, L.; Gao, P. Particle swarm optimization fractional slope entropy: A new time series complexity indicator for bearing fault diagnosis. *Fractal Fract.* **2022**, *6*, 345. [[CrossRef](#)]
38. Li, W.; Zhang, L.; Chen, X.; Wu, C.; Cui, Z.; Niu, C. Predicting the evolution of sheet metal surface scratching by the technique of artificial intelligence. *Int. J. Adv. Manuf. Technol.* **2021**, *112*, 853–865. [[CrossRef](#)]
39. Gao, Y.; Zhao, T.; Zheng, Z.; Liu, D. A Cotton Leaf Water Potential Prediction Model Based on Particle Swarm Optimisation of the LS-SVM Model. *Agronomy* **2023**, *13*, 2929. [[CrossRef](#)]
40. Zhang, Y.; Lu, Y.; Zhang, J. Research on numerical control machine fault diagnosis based on distribution adaptive one-dimensional convolutional neural network. *J. Phys. Conf. Ser.* **2021**, *1948*, 012105.
41. Zong, S.; Wang, S.; Luo, Z.; Wu, X.; Zhang, H.; Ni, Z. Robust Damage Detection and Localization Under Complex Environmental Conditions Using Singular Value Decomposition-based Feature Extraction and One-dimensional Convolutional Neural Network. *Chin. J. Mech. Eng.* **2023**, *36*, 61. [[CrossRef](#)]
42. Gautam, A.K.; Tariq, M.; Verma, K.S.; Pandey, J.P. An intelligent BWO algorithm-based maximum power extraction from solar-PV-powered BLDC motor-driven light electric vehicles. *J. Intell. Fuzzy Syst.* **2022**, *42*, 767–777. [[CrossRef](#)]
43. Guo, T.; Xu, F.; Ma, J.; Ge, F. Component Prediction of Antai Pills Based on One-Dimensional Convolutional Neural Network and Near-Infrared Spectroscopy. *J. Spectrosc.* **2022**, *2022*, 6875022. [[CrossRef](#)]
44. National Park Service. Available online: <https://www.nps.gov/glba/learn/nature/soundclips.htm> (accessed on 29 June 2023).

Disclaimer/Publisher’s Note: The statements, opinions and data contained in all publications are solely those of the individual author(s) and contributor(s) and not of MDPI and/or the editor(s). MDPI and/or the editor(s) disclaim responsibility for any injury to people or property resulting from any ideas, methods, instructions or products referred to in the content.